



15th Canadian Masonry Symposium
Ottawa, Canada
June 2-5, 2025



Damage From Ups and Downs: Investigating Cracking in Unreinforced Masonry Structures Exposed to Settlement and Uplift Cycles Using Finite Element Analyses

Alfonso Prosperⁱ, Michele Longoⁱⁱ, Paul A. Korswagenⁱⁱⁱ, Mandy Korff^{iv} and Jan G. Rots^v

ABSTRACT

Cycles of settlement and uplift beneath existing masonry structures can lead to visible cracks, which not only affect the aesthetic appearance and functionality of the building but can also compromise its structural integrity and undermine the occupants' sense of safety. These cyclic ground movements can be triggered by seasonal actions, such as fluctuation in the groundwater table. In the Netherlands, many existing masonry structures on shallow foundations rest directly on the subsurface, making them vulnerable to cyclic ground movements. Settlement and uplift cycles cause “breathing” masonry cracks, which open and close over time without fully sealing. This study uses finite element analyses to investigate and assess the damage of structures subjected to cyclic quasi-static ground movements. A case study is presented for the analysis, featuring the geometry of an existing low-rise masonry structure with an age exceeding 50 years. A 3D non-linear shell-element model is used to evaluate the structural response, featuring an unreinforced strip foundation and including the non-linear tensile softening and cracking behaviour of masonry. Heaving and sinking displacements are applied to a non-linear interface simulating the soil-foundation interaction at the bottom of the strip foundation. The intensity of the ground displacements is quantified by their angular distortion. A damage parameter objectively assesses the severity of damage by considering the number, length, and width of cracks. Results indicate that repeated cycles of settlement (and uplift) have been observed to cause irreversible cracking damage in the model, with crack widths ranging from 1 to 5 mm, progressively increasing over time. Damage occurring during settlement is, on average, twice as severe as that during uplift. Overall, cycles of settlement and uplift may induce cracking damage up to twice as high as that caused by cycles of settlement alone, depending on the magnitude and shape of the ground movements.

KEYWORDS

Settlement, uplift, cyclic ground movements, unreinforced masonry, cracking damage, damage assessment, finite elements

ⁱ Postdoc Researcher, Delft University of Technology, Delft, The Netherlands, A.Proseri@tudelft.nl

ⁱⁱ Researcher, Delft University of Technology, Delft, The Netherlands, M.Longo@tudelft.nl

ⁱⁱⁱ Assistant Professor, Delft University of Technology, Delft, The Netherlands, P.A.KorswagenEguren@tudelft.nl

^{iv} Associate Professor, Delft University of Technology, Delft, The Netherlands, M.Korff@tudelft.nl

^v Full Professor, Delft University of Technology, Delft, The Netherlands, J.G.Rots@tudelft.nl



INTRODUCTION

Quasi-static ground movements beneath buildings develop gradually over time and are not linked to dynamic or transient processes. These movements involve both settlement (downward displacement) and uplift (upward displacement) of the ground surface, depending on the underlying triggering mechanisms. While some drivers, such as consolidation of saturated soils, tectonic deformation, creep and organic matter decomposition, and other long-term processes trigger irreversible changes in the ground surface, other causes can trigger cyclic and periodic ground movements, such as seasonal changes in the groundwater table levels, cycles of clay shrinkage and swelling or seasonal extraction of underground resources. In this context, structures resting on the subsurface are subjected to cyclic ground movements, which can lead to varying degrees of damage. This damage often manifests as visible cracks in walls, resulting from repeated stress and strain on the structural elements. Structures constructed with brittle materials, such as unreinforced masonry, are particularly susceptible to damage from both settlement and uplift. These movements generate tensile stresses within the structure, often leading to the formation of cracks. In the Netherlands, approximately 70% of structures are estimated to be built on shallow foundations [1], meaning they rest directly on the upper soil layers and are therefore susceptible to ground movements. The Western and Northern areas of the country are widely known for the widespread presence of subsidence processes, triggered by various overlapping natural and anthropogenic causes combined with the presence of highly compressible clay and peat soils. Such “soft soil” predisposes the occurrence of cycles of settlement and uplift, due to the seasonal variations in the groundwater table, a situation that is further exacerbated by more frequent and severe droughts and rains due to climate change. Prior studies have investigated the damage to structures induced by subsidence using numerical analyses [2-8]. Computational models idealize the behaviour of existing structures and provide insight into their response, especially when observations and measurements of such buildings may be limited or unavailable.

This paper demonstrates the use of finite elements to assess the cracking damage of existing unreinforced masonry structures on strip foundations subjected to cycles of settlement and uplift. The existing modelling strategies are herein further refined to account for the cyclical occurrence of subsidence and heave and to evaluate their effects. The methodology, originally inspired by quasi-static in-plane testing of masonry walls under bilateral displacement, is adapted to consider instead vertical ground movements, including both upward and downward displacements.

METHODOLOGY AND SETUP OF COMPUTATIONAL MODELS

In this study, a 3D model of an existing unreinforced masonry building is used for the analyses carried out with the finite element software DIANA 10.8 [9]. The model represents a farmhouse built in 1883, already studied in prior research [3, 6, 7, 10] (Figure 1). The building has double wythe façades (thickness of 210 mm). The features of the adopted modelling strategy are listed below:

- Façade and walls: a 3D model of half of the building, due to its structural symmetry, is used, without explicit modelling of floors (only their weight is included) and party walls [11, 12]. The model includes the transversal walls and foundations, which were observed to influence the response of 3D models to settlement in prior research [11, 12].
- Strip foundation: unreinforced masonry strip foundations underneath the façade and the transversal walls are included. The strip foundation is characterized by a stepped cross-section, with the base gradually increasing in size, varying between 300 mm, 500 mm, and 700 mm.
- Non-linear masonry material: The non-linear orthotropic behaviour of the masonry material is modelled using the Engineering Masonry Model (EMM) [13, 14]. EMM incorporates horizontal and vertical tensile softening, along with shear softening. Tension unloading follows a secant

approach, while shear unloading is modelled elastically. The EMM uses predefined crack orientations, making it particularly effective for modelling masonry, composed of units, bed joints, and head joints [15]. The values of the material properties are reported in Table 1 [13, 16, 17]. A running bond is considered for the masonry. The same material model is used for the lintel, but with rotated local axes of 90 degrees (soldier bond masonry). The crack bandwidth is determined using Govindjee 's projection method [18, 19].

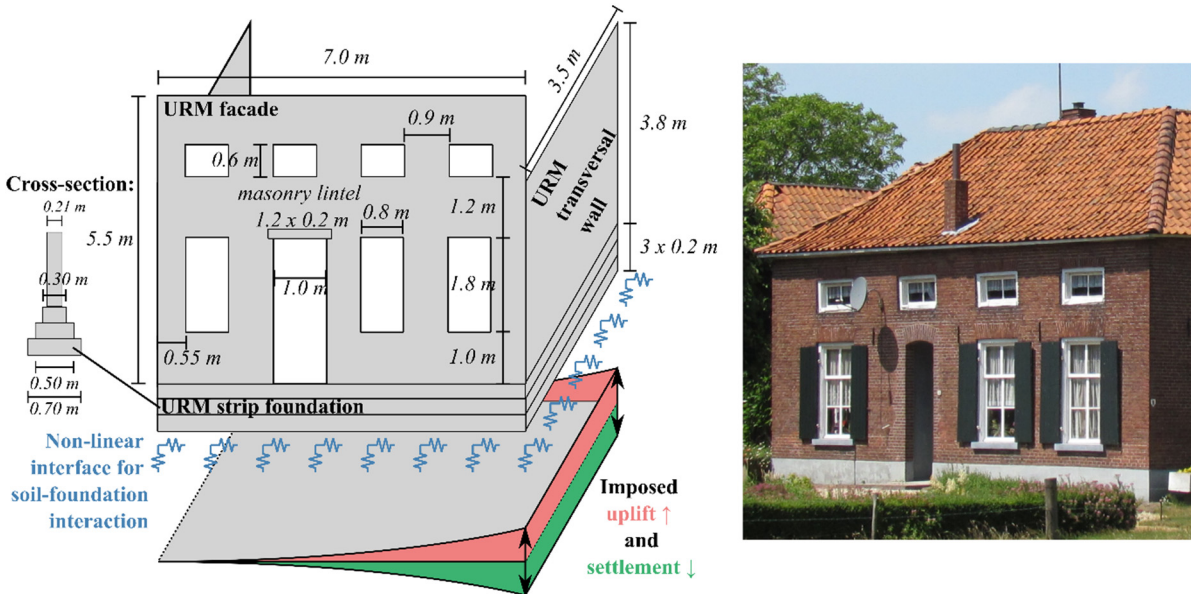


Figure 1: The left image schematically illustrates the 3D modelling approach. The right photo depicts a typical farmhouse façade as an example, retrieved from [10, 20].

- Soil-foundation interaction: The interaction between the soil and the foundation is modelled using interfaces, based on the approach implemented in previous studies ([2, 4, 11, 12]). The interface follows Coulomb-friction behaviour, with vertical and horizontal stiffness values determined using the formulations provided by [21, 22], which depend on the soil's shear modulus “G,” Poisson's ratio “ ν ,” and the foundation's base width “B” and length “L”. With the Coulomb-friction interface, tangential forces become zero when tension is applied. For pure traction, the interface has zero strength. The soil material considered is “Clay”, with a shear modulus “G” of 10 MPa, Poisson's ratio “ ν ” equal to 0.45 and a friction angle of 15°.
- Finite element discretization: Shell elements are used for the façade, transversal walls, lintel, and strip foundations. Quadratic 8-node quadrilateral and 6-node triangular elements are applied to the walls, lintel, and foundation, with 2x2 Gaussian integration for the quadrilateral elements and 3 integration points for the triangular elements. 3 integration points are used across the thickness of the elements [11, 12]. Interfaces are modelled with 3+3 node elements.
- Gravity and overburden: The model accounts for the self-weight of the structure. Additionally, distributed forces of 2.53 N/mm are applied above the transverse walls to represent the weight of a timber roof. Gravity and overburden are included in the analyses through 10 load steps each, with a maximum of 1000 iterations per step using the Secant (quasi-Newton) method, which uses the stiffness matrix from the previous step's final iteration. Convergence criteria for energy, displacement, and force are applied with tolerances of 10^{-4} , 10^{-5} , and 10^{-3} , respectively. While convergence across all norms is required, non-convergence steps are permitted.

- Cracking damage assessment: Crack initiation and progression are evaluated through the parameter Ψ , which consolidates crack length, number, and width into a single value [15, 23]. The parameter Ψ was computed considering the output of the façade only. A summary of the relation between Ψ and the approximate crack width for the various damage levels is presented in Table 2. Ψ is best suited for assessing “light damage”, i.e., up to cracks of about 5 mm wide, whereas damage that could affect the structural safety would require a different metric. It is important to note that the association of Ψ and different degrees of damage is fuzzy, as the latter is not entirely objective [15].

Table 1: The material properties adopted in the models for the masonry material

Material Properties	Symbol	Unit of measure	Value
Young’s modulus vertical direction	E_y	MPa	5000
Young’s modulus horizontal direction	E_x	MPa	2500
Shear Modulus	G_{xy}	MPa	2000
Bed joint tensile strength	f_{ty}	MPa	0.100
Minimum strength head-joint	$f_{tx,min}$	MPa	0.150
Fracture energy in tension	$G_{t,I}$	N/m	10.0
Angle between stepped crack and bed-joint	α	rad	0.5
Compressive strength	f_c	MPa	8.50
Fracture energy in compression	G_c	N/mm	18.39
Friction angle	ϕ	rad	0.64
Cohesion	c	MPa	0.150
Fracture energy in shear	G_s	N/mm	0.100
Mass Density	ρ	Kg/m ³	1900

Table 2: Damage scale with the classification of visible damage and the corresponding discretization of the damage parameter Ψ , from [15, 23-25].

Damage level	Degree of damage	Approximate crack width	Parameter of damage
DL0	No Damage	Imperceptible cracks	$\Psi < 1$
DL1	Negligible	up to 0.1 mm	$1 \leq \Psi < 1.5$
DL2	Very slight	up to 1 mm	$1.5 \leq \Psi < 2.5$
DL3	Slight (end of light damage)	up to 5 mm	$2.5 \leq \Psi < 3.5$
<i>DL4</i>	<i>Moderate (No longer light damage)</i>	<i>5 to 15 mm</i>	<i>$3.5 \leq \Psi < 4.5$</i>
<i>DL5</i>	<i>Severe</i>	<i>15 to 25 mm</i>	<i>$4.5 \leq \Psi < 6.0$</i>
<i>DL6</i>	<i>Very Severe</i>	<i>Above 25 mm</i>	<i>$\Psi \geq 6.0$</i>

Applied settlement and uplift shapes and loading protocols

In the FE models, settlement and uplift are imposed at the bottom of the non-linear interface. In this study, two shapes are considered for the analyses: **symmetric** and **asymmetric hogging** (in Figure 2a and b respectively). The two scenarios illustrate two possible downward displacements of the façade sides, while the transverse walls move uniformly due to the absence of 3D variation. The same shapes apply to uplift, but in reverse, causing the façade sides to move upward. The magnitude of the settlement and uplift is quantified by the maximum angular distortion, i.e. the slope of the line connecting two points relative to the tilt of the building [26], along the imposed displacement profiles. In this study, "applied" settlements are distinguished from "measured" displacements at the bottom of the façade [2, 27]. The distortion β at the

interface is labelled as "applied β ," while "measured β " is calculated from the displacements at the façade base. The vertical displacement of each settlement shape is scaled to ensure that the applied angular distortion matches the desired value. To investigate the effects of repetitions of settlement and uplift, loading protocols are defined, drawing inspiration from those used in in-plane quasi-static tests of masonry walls [15].

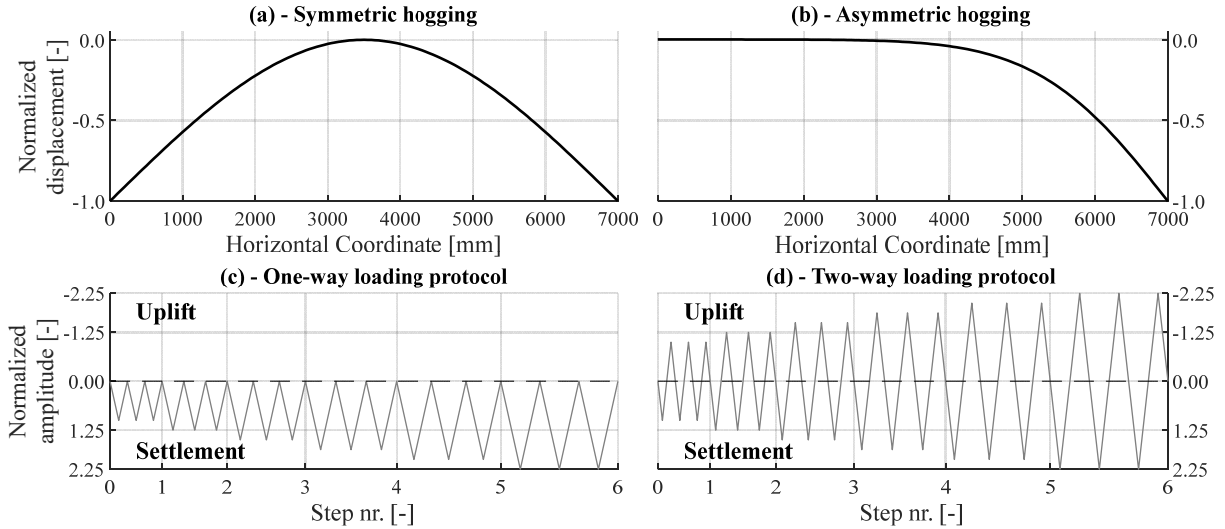


Figure 2: The imposed settlement shapes: (a) symmetric hogging and (b) asymmetric hogging. The adopted loading protocols are (c) one-way and (d) two-way.

While in-plane quasi-static tests typically involve the application of bi-directional horizontal displacements, this study focuses on settlement and uplift. Therefore, the following definitions are adapted for this research:

- **Cycle:** refers to a single application of a load-unload pattern, which may involve only settlement, only uplift, or a single sequence of settlement followed by uplift. During uplift, a negative load is applied, reversing the settlement shapes and causing the façade side(s) to rise upward, in contrast to the downward movement applied during settlement.
- **Step:** comprises one or more cycles. Subsequent steps progressively increase in magnitude throughout the load protocols. It is important to note that "steps" in the context of loading protocols should not be confused with "load steps" in finite element (FE) analyses, as the latter refers to the number of steps used to apply a load during simulations.
- **Load protocol:** Predefined sequence of steps applied during loading.

The two selected loading protocols are defined as follows to characterize the cyclic displacements: i) “**One-way**” protocol (Figure 2c), in which only settlement and unloading are applied in each cycle, and ii) “**Two-way**” protocol (Figure 2d), in which an alternation of settlement, unloading, uplift and unloading alternate in each cycle, with the intensity of the uplift set to match that of the settlement. For the defined loading protocols, the very first angular distortion amplitude needs to be defined. The remaining steps follow from this first with a constant increase of 25% for normalised amplitudes of 1.00, 1.25, 1.50, 1.75, 2.00, and 2.25 for up to six steps (Figure 2c and d), following the approach used for in-plane quasi-static tests of masonry walls [15]. The first amplitude was determined through two preliminary “monotonic” analyses, where each settlement shape was applied without unloading until an angular distortion of 1/500 was reached. The monotonic settlement is applied with the same iteration procedures used for gravity and overburden, however, only the energy norm is used. The selected load step size is 0.01 mm/step, which

means that the maximum settlement of the settlement profile is increased in steps of 0.01 mm up to the target angular distortion. This corresponds to 450 (up to 4.5 mm) and 460 steps (up to 4.6 mm) for the symmetric and asymmetric hogging respectively. For each settlement shape, the angular distortion that induced a Ψ equal to 1.0 (crack width of 0.1 mm) was considered to define the first amplitude of the loading protocols. This corresponds to the values 1/1250 and 1/602 for symmetric and asymmetric hogging respectively. The maximum angular distortion values of the loading protocols correspond to 1/555 (2.25x1/1250) and 1/268 (2.25x1/602) for symmetric and asymmetric hogging. For each step of the loading protocols, 3 cycles are used to investigate the effect of multiple repetitions with the same intensity.

RESULTS

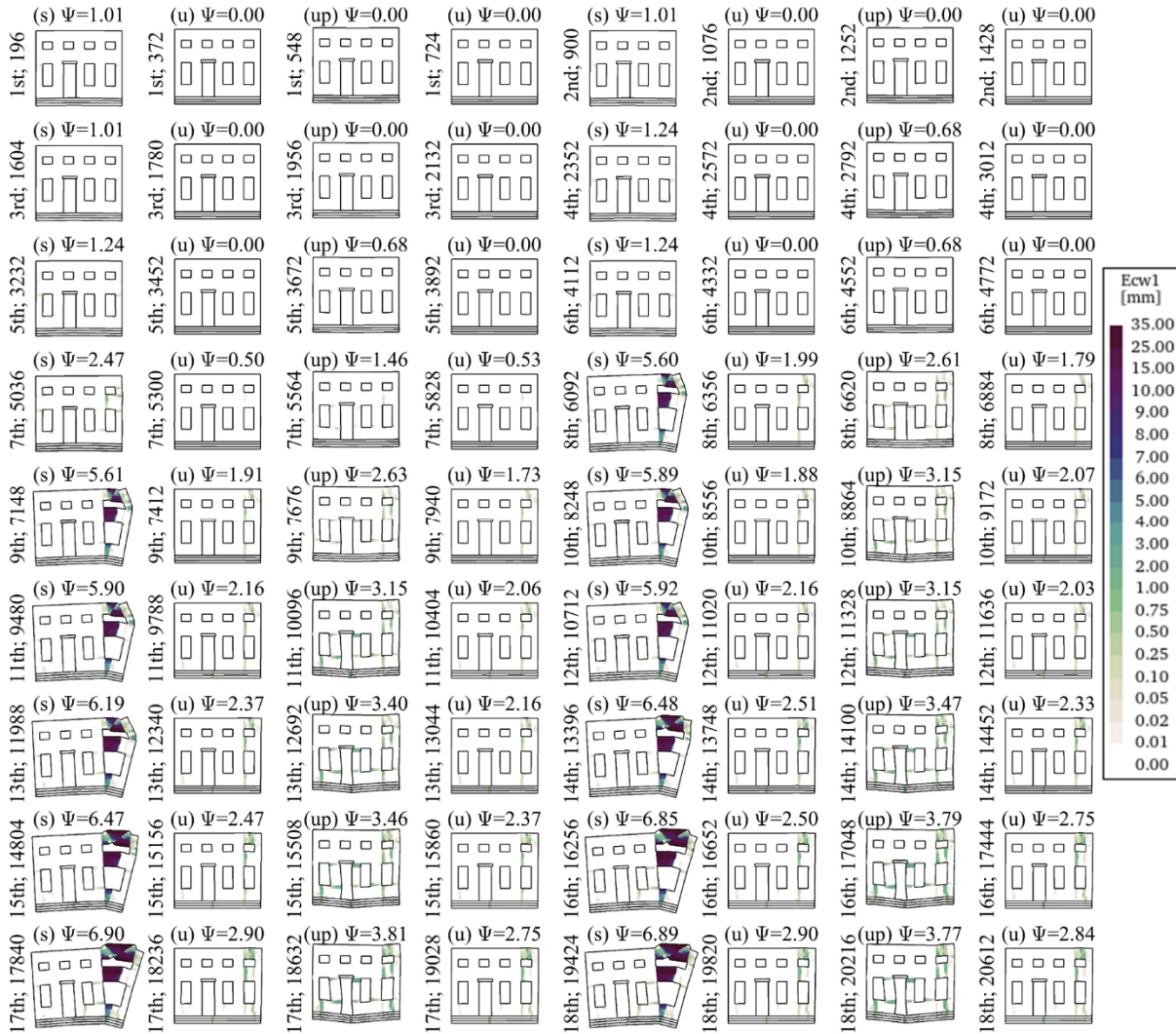


Figure 3: The crack patterns under symmetric hogging using a two-way loading protocol. Each plot displays the cycle number, corresponding load step from the FE analysis, and the Ψ value at the top. The four phases of each cycle, settlement (s), unloading (u), uplift (up), and unloading (u), are labelled before each Ψ value. Contour plots show the maximum principal crack width (E_{cw1}), with deformation magnified by a factor of 100.

Figure 3 presents the crack patterns for symmetric hogging and the two-way loading protocol for each cycle. The corresponding Ψ value is shown for each plot. Damage aggravates with the progressive increase in the applied distortion. Cracks initiate around the windows and progress mainly vertically or horizontally, as a result of using the EMM [2, 15, 28]. Similar crack patterns can be observed in real structures due to settlement and uplift [29]. For each cycle, damage is visibly less severe in uplift than in settlement. During the first cycles, cracks open and close without any residual Ψ i.e., residual damage observable at the end of the unloading. Residual Ψ values are observable from the 7th cycle, corresponding to the beginning of the 3rd step of the loading protocol. At this point, cracks remain open and do not fully close during unloading, indicating a shift towards permanent damage.

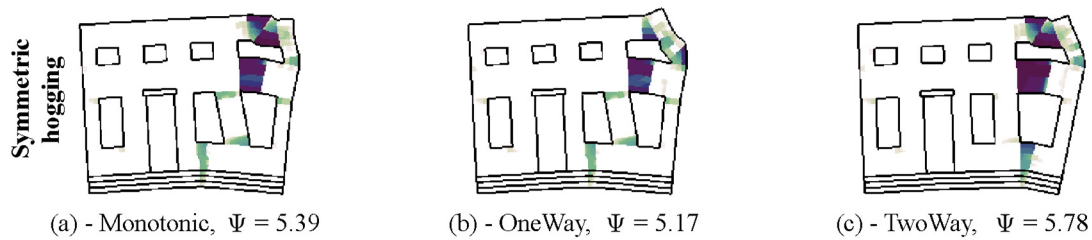


Figure 4. Comparison of the crack patterns for symmetric hogging, monotonic against loading protocols under applied angular distortion β equal to 1/750. Contour plots show the maximum principal crack width (E_{cr1}), with deformation magnified by a factor of 100. The legend is the same as shown in Figure 3.

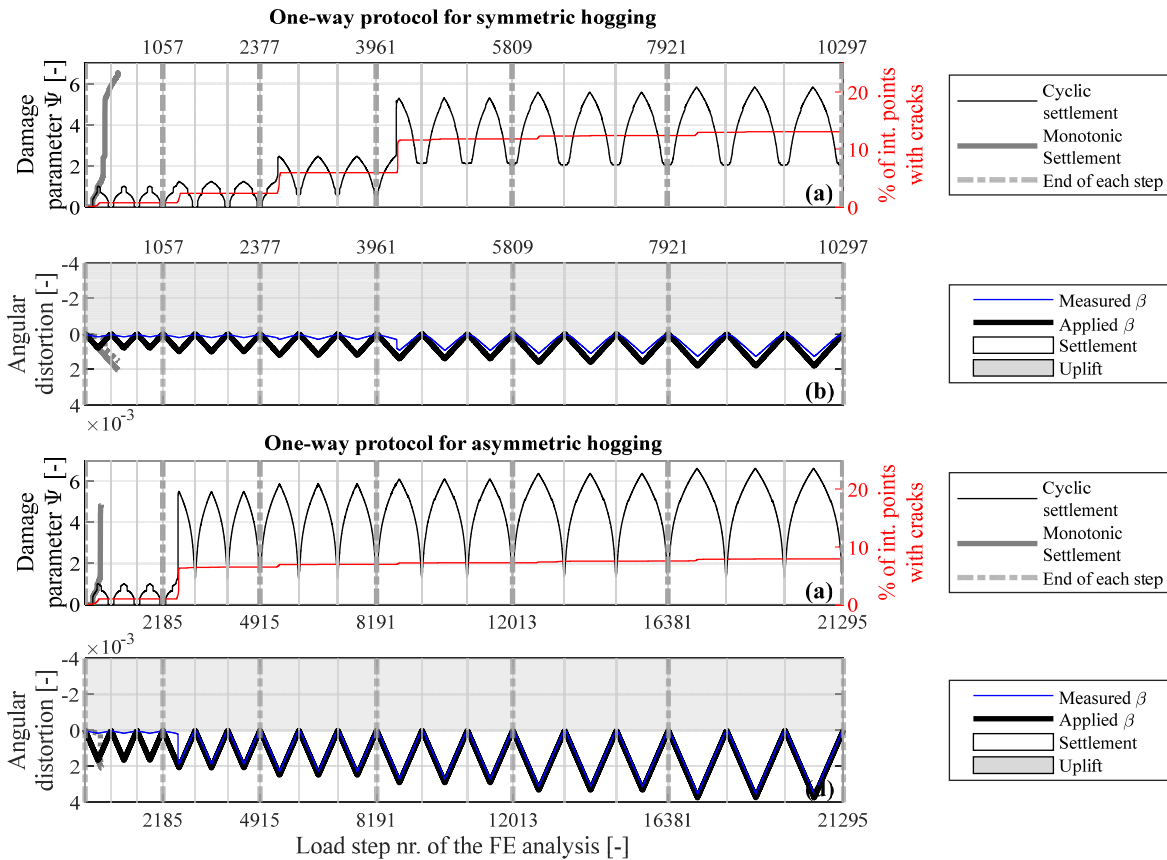


Figure 5: Results for the one-way protocol, load step number against angular distortion β and the damage Ψ : (a) and (b) for symmetric, and (c) and (d) for asymmetric hogging.

Figure 4 shows a comparison between the crack pattern of the monotonic analysis and the ones of the loading protocols subjected to symmetric hogging under an applied angular distortion of $1/750$. Figure 4b, c display the crack patterns at the point where the distortion is reached for the first time. Although in all three analyses, the damage is localized in the right part of the façade, the width, location and length of the cracks are influenced by the applied load, particularly in the top-right portion of the façade. As a result, the crack pattern differs between settlement (and uplift) cycles compared to monotonic settlement.

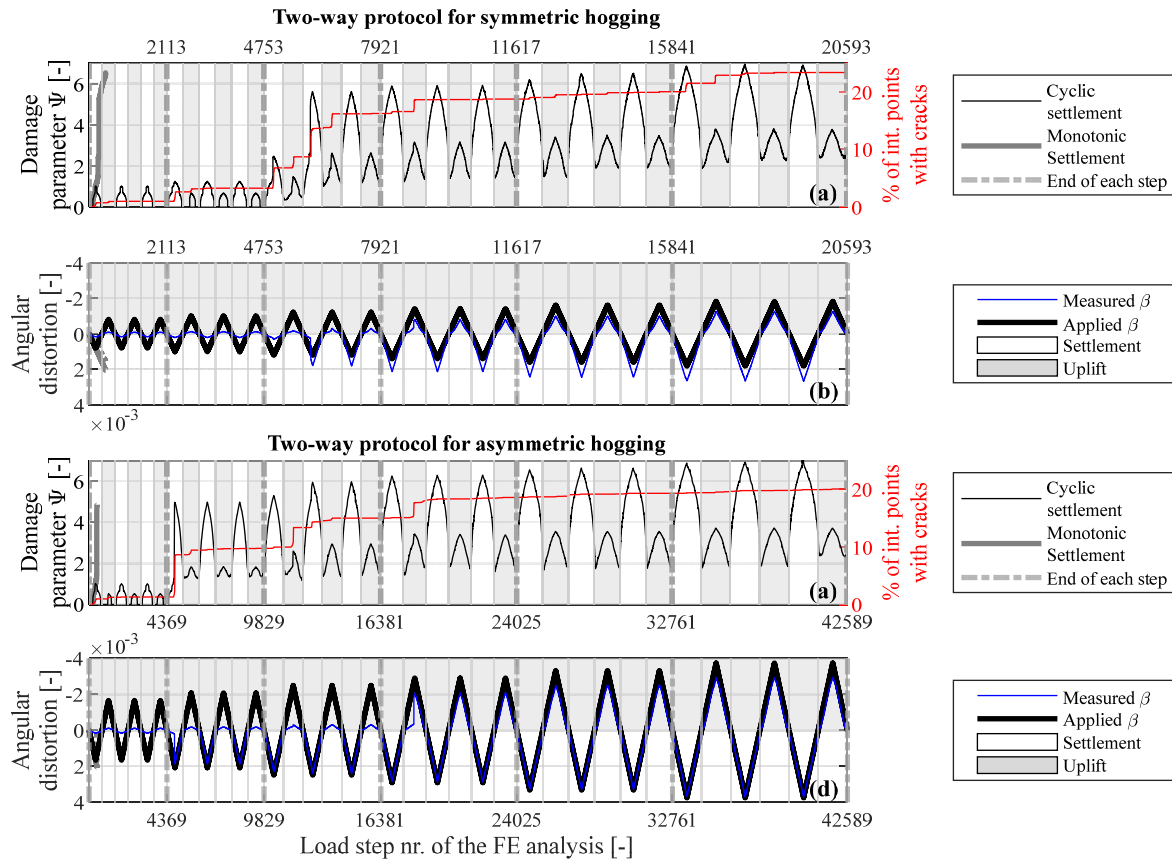


Figure 6: Results for the two-way protocol, load step number against angular distortion β and the damage Ψ : (a) and (b) for symmetric, and (c) and (d) for asymmetric hogging.

However, visually examining the cracking alone offers limited insight into the progression of damage in the model. Therefore, the damage parameter Ψ can be plotted against the load step of the FE analyses, as illustrated in Figure 5a, c for the one-way protocol and Figure 6a, c for the two-way protocol. In the same panels, secondary y-axes are used to display the percentage of integration points in which cracking occurs during the analysis. In real structures, cracks may close but rarely fully seal unless self-healing processes occur [30], and thus the structural behaviour inevitably differs from its original state. While the trends of Ψ against the load steps reflect visual damage, the percentage of integration points with cracks indirectly illustrates how damage progressively aggravates throughout the analyses. Figure 5b, d and Figure 5b, d show the evolution of both the applied and measured angular distortions. The measured distortion is computed from the displacements at the top edge of the strip foundation in the model, providing a representation of the façade's deformation. Overall, the measured angular distortion is always lower than the applied one. However, in the case of symmetric hogging, the measured angular distortion becomes higher than the imposed one. This happens because cracks propagate through the top edge of the strip foundation (Figure 3), affecting the computed values of the measured angular distortion.

In both Figure 5 and Figure 6, the results of the preliminary monotonic analyses are shown. For each step and each loading protocol, the maximum and residual Ψ values are reported in Table 3. For all the loading protocols, the results closely follow the ones of the monotonic analyses during the first cycle, as settlement is applied before the first unloading. The results show how damage progressively aggravates as new cracks open (as shown by the trends of the cracked integration points). For both one- and two-way protocols, new cracks primarily open in the first cycle of each step, when the applied distortion is increased. Overall, the

maximum Ψ values for two-way protocols are observed to be either nearly equal to or up to 2.3 times higher than their counterparts in one-way protocols, depending on the specific step considered, with the difference becoming more pronounced as the applied distortion increases. Notably, the differences in residual damage are even more significant, ranging from 15% to 240% higher for the two-way protocol, except for Step 4 in symmetric hogging, where the increase is only 4%.

Figure 6 shows how the cracking of the two-way loading protocols evolves during both settlement (positive distortions) and uplift (negative distortions). For each cycle, the damage in settlement is 1.5 to 3.0 times higher than the damage during uplift. For the selected hogging shapes, downward displacement is expected to induce tensile stresses at the top of the façade, leading to more severe cracking compared to the uplift case. In contrast, during uplift, tensile stresses develop at the bottom of the façade, where the foundation increases stiffness and counteracts crack formation. Additionally, this research assesses damage solely based on cracking in the façade and does not account for any cracks that may develop in the strip foundation during uplift. However, examining the percentage of integration points in which cracks occurred reveals that new cracks form during uplift, causing the damage to progressively aggravate throughout the analyses. Thus, even if during uplift the visual damage is less severe than in settlement, it leads to the formation of new cracks and exacerbates the overall damage. Residual damage accumulates from the second step for asymmetric hogging and the third one for the symmetric hogging for both one- and two- ways protocols. In both cases, the residual damage is observed once the models have reached or exceeded Ψ equal to 2.0 (cracks up to 1 mm). In one-way loading protocols, residual damage does not accumulate progressively. In contrast, it continuously increases with each step in two-way protocols (Table 3).

For both loading protocols, it can be observed that when the model achieves Ψ values higher than 5.0, the relative increment of maximum Ψ decreases as the load amplitude increases (Table 3). Conversely, for two-way protocols, the residual damage and its relative increment increase. This is, however, not the case for one-way protocols, in which the residual damage is also stable. In other words, for two-way protocols as the maximum damage stabilizes, the structure exhibits progressively more irreversible (residual) damage, leading to larger increments in residual Ψ with each step.

DISCUSSION AND CONCLUSIONS

This research highlights the impact of settlement and uplift cycles on building damage, emphasizing the importance of including cyclic behaviour in damage assessments rather than focusing solely on settlement or uplift. Non-linear finite element analyses are used to study cracking. Loading protocols applied to the models idealize repeated cycles of settlement and uplift of increasing magnitudes. Further research is recommended to examine the effects of 3D variations in settlement and uplift patterns, additional loading protocols, and different structural typologies. The relationship between the protocol and the causes of settlement and uplift also requires further investigation. The results of the analyses showed that:

- Repeated cycles of settlement (and uplift) progressively form new cracks, which deteriorate the structural response and lead to damage aggravation.
- The irreversible cracking caused by the repetition of settlement (and uplift) has been observed to result in crack widths ranging from 1 to 5 mm, progressively increasing over time.
- Cycles of settlement and uplift can cause cracking that is nearly equal to or more than twice as severe as that caused by settlement cycles alone, depending on the magnitude of the applied distortion.
- For the same imposed distortion, cracking damage occurring during settlement is approximately 1.5 to 3.0 times higher than that observed during uplift.

Table 3: Values of the maximum and residual Ψ . The increment per step is reported and calculated relative to the values of the previous step.

Step	Normalized amplitude	Maximum Ψ value [-]							
		Symmetric hogging				Asymmetric hogging			
		One-Way		Two-Way		One-Way		Two-Way	
		Value	Increase	Value	Increase	Value	Increase	Value	Increase
1	1.00	1.01	-	1.01	-	1.01	-	1.01	-
2	1.25	1.24	+23%	1.24	+23%	5.51	+446%	4.98	+394%
3	1.50	2.46	+98%	5.61	+353%	5.87	+7%	5.97	+20%
4	1.75	5.03	+105%	5.92	+5%	6.11	+4%	6.30	+5%
5	2.00	5.58	+11%	6.48	+10%	6.38	+4%	6.64	+5%
6	2.25	5.84	+5%	6.90	+7%	6.63	+4%	7.05	+6%
Step	Normalized amplitude	Residual Ψ value [-]							
		Symmetric hogging				Asymmetric hogging			
		One-Way		Two-Way		One-Way		Two-Way	
		Value	Increase	Value	Increase	Value	Increase	Value	Increase
1	1.00	0.00	-	0.00	-	0.00	-	0.00	-
2	1.25	0.00	-	0.00	-	1.25	-	1.61	-
3	1.50	0.50	-	1.73	-	1.26	+1%	1.78	+11%
4	1.75	1.95	-	2.03	+17%	1.35	+7%	2.31	+30%
5	2.00	2.04	+4%	2.37	+17%	1.33	-1%	2.59	+12%
6	2.25	2.01	-1%	2.84	+20%	1.31	-2%	3.13	+21%

REFERENCES

- [1] The Council for the Environment and Infrastructure (Rli), (2024), "Goed Gefundeerd: advies om te komen tot een nationale aanpak funderingsproblematiek."
- [2] Prosperi, A., Longo, M., Korswagen, P.A., Korff, M., and Rots, J.G. (2023), "Sensitivity modelling with objective damage assessment of unreinforced masonry façades undergoing different subsidence settlement patterns," *Eng Struct*, vol. 286, p. 116113.
- [3] Rots, J.G., Korswagen, P.A., and Longo, M., (2021), "Computational modelling checks of masonry building damage due to deep subsidence," Delft University of Technology, February 19, 202, vol. Report number 01, Version 05.
- [4] Prosperi, A., Longo, M., Korswagen, P.A., Korff, M., and Rots, J.G. (2023), "Shape matters: Influence of varying settlement profiles due to multicausal subsidence when modelling damage in a masonry façade," in *Tenth International Symposium on Land Subsidence 2023*, of Conference.
- [5] Fuertes, J. (2024), "Calibrated Numerical models for masonry buildings subjected to subsidence-related ground settlements," Civil Engineering & Geosciences, Delft University of Technology. [Online]. Available: <https://resolver.tudelft.nl/uuid:b35ef3f8-48d8-46ed-861e-774632bf238b>
- [6] Korswagen, P., Longo, M., Rots, J., and Prosperi, A., ""Supporting analyses to determine probability of damage and fragility curves due to indirect subsidence effects". Delft University of Technology. Report. October 3, 2022."
- [7] Korswagen, P., Longo, M., Rots, J., and Prosperi, A., " "Appendixes to supporting analyses to determine probability of damage and fragility curves due to indirect subsidence effects". Delft University of Technology. Report, 2022.."
- [8] Ferlisi, S., Nicodemo, G., Peduto, D., Negulescu, C., and Grandjean, G. (2020), "Deterministic and probabilistic analyses of the 3D response of masonry buildings to imposed settlement troughs," (in English), *Georisk*, vol. 14, no. 4, pp. 260-279, Oct 1, doi: 10.1080/17499518.2019.1658880.
- [9] DIANA FEA bv, (2023), "Theory Manual (DIANA 10.8)," Thijsseweg 11, 2629 JA Delft, The Netherlands.

- [10] Korswagen, P.A., Longo, M., Prosperi, A., Rots, J.G., and Terwel, K.C. (2023), "Modelling of Damage in Historical Masonry Façades Subjected to a Combination of Ground Settlement and Vibrations," in *International Conference on Structural Analysis of Historical Constructions*, of Conference: Springer, pp. 904-917.
- [11] Prosperi, A., Longo, M., Korswagen, P.A., Korff, M., and Rots, J.G. (2024), "2D and 3D Modelling Strategies to Reproduce the Response of Historical Masonry Buildings Subjected to Settlements," *Int J Archit Herit*, pp. 1-17.
- [12] Prosperi, A., Longo, M., Korswagen, P.A., Korff, M., and Rots, J.G. (2023), "Accurate and Efficient 2D Modelling of Historical Masonry Buildings Subjected to Settlements in Comparison to 3D Approaches," in *International Conference on Structural Analysis of Historical Constructions*, of Conference: Springer, pp. 232-244.
- [13] Schreppers, G., Garofano, A., Messali, F., and Rots, J. (2016), "DIANA validation report for masonry modelling," *DIANA FEA report*.
- [14] Rots, J., Messali, F., Esposito, R., Jafari, S., and Mariani, V. (2016), "Thematic Keynote Computational modelling of masonry with a view to Groningen induced seismicity," in *Structural Analysis of Historical Constructions: Anamnesis, Diagnosis, Therapy, Controls: Proceedings of the 10th International Conference on Structural Analysis of Historical Constructions (SAHC, Leuven, Belgium, 13-15 September 2016)*, of Conference: CRC Press, pp. 227-238.
- [15] Korswagen, P.A. (2024) *Quantifying the probability of light damage to masonry structures: An exploration of crack initiation and progression due to seismic vibrations on masonry buildings with existing damage* (Dissertation (TU Delft)). Delft University of Technology.
- [16] *Assessment of structural safety of buildings in case of erection, reconstruction and disapproval - Induced earthquakes - Basis of design, actions and resistances*, NPR9998:2020en, April 1 2021.
- [17] Korswagen, P.A., Longo, M., Meulman, E., and van Hoogdalem, C. (2017), "Damage sensitivity of Groningen masonry structures—Experimental and computational studies: Stream 1."
- [18] Govindjee, S., Kay, G.J., and Simo, J.C. (1995), "Anisotropic modelling and numerical simulation of brittle damage in concrete," *International journal for numerical methods in engineering*, vol. 38, no. 21, pp. 3611-3633.
- [19] DIANA FEA by, (2024), "Finite element analysis user's manual - release 10.8," Laan van Waalhaven 462, 2497 GR, The Hague, The Netherlands.
- [20] "Monumental Farmhouse, National Monument ID: 523688." <https://rijksmonumenten.nl/monument/523688/boerderij-met-aangrenzende-bijschuren/breedenbroek/> (accessed November, 2024).
- [21] NEHRP, (2012), "NIST GCR 12-917-21 Soil–structure interaction for building structures," National Institute of Standards and Technology, US Department of Commerce, Gaithersburg.
- [22] Gazetas, G., "Foundation vibrations," in *Foundation engineering handbook*: Springer, 1991, pp. 553-593.
- [23] Korswagen, P.A., Longo, M., Meulman, E., and Rots, J.G. (2019), "Crack initiation and propagation in unreinforced masonry specimens subjected to repeated in-plane loading during light damage," *Bulletin of Earthquake Engineering*, vol. 17, no. 8, pp. 4651-4687.
- [24] Burland, J.B., Broms, B.B., and De Mello, V.F. (1978), "Behaviour of foundations and structures."
- [25] Grünthal, G., (1998), "European macroseismic scale 1998," European Seismological Commission (ESC).
- [26] Burland, J.B. and Wroth, C., (1975), "Settlement of buildings and associated damage."
- [27] Prosperi, A. (2025) *Modelling of subsidence induced damage to masonry buildings: Influence of soil heterogeneity on settlement and development of fragility curves* (Dissertation (TU Delft)). Delft University of Technology.
- [28] Sousamli, M. (2024), "Orthotropic Cyclic Continuum Constitutive Model For Masonry Structures And Comparative Studies."
- [29] De Vent, I.A.E. (2011), "Prototype of a diagnostic decision support tool for structural damage in masonry."

[30] Gaggero, M.B., Korswagen, P.A., Esposito, R., and Rots, J.G. (2024), "Innovative Application of Self-healing Technology to Masonry: A Proof of Concept," *Int J Archit Herit*, pp. 1-11.